PROTEINS: Structure, Function, and Genetics 13:336–351 (1992)

The Refined Crystal Structure of *Pseudomonas putida* Lipoamide Dehydrogenase Complexed With NAD^+ at 2.45 Å Resolution

Andrea Mattevi,[1] Galya Obmolova,[1] John R. Sokatch,[2] Christian Betzel,[3] and Wim G.J. Hol[1]
[1]BIOSON Research Institute, Department of Chemistry, University of Groningen. 9747 AG Groningen, The Netherlands; [2]Department of Biochemistry and Molecular Biology, The University of Oklahoma Health Sciences Center, Oklahoma City, Oklahoma 73190; and [3]EMBL Outstation, 2000 Hamburg 52, Federal Republic of Germany

ABSTRACT **The three-dimensional structure of one of the three lipoamide dehydrogenases occurring in *Pseudomonas putida*, LipDH Val, has been determined at 2.45 Å resolution. The orthorhombic crystals, grown in the presence of 20 mM NAD^+, contain 458 residues per asymmetric unit. A crystallographic 2-fold axis generates the dimer which is observed in solution. The final crystallographic *R*-factor is 21.8% for 18,216 unique reflections and a model consisting of 3,452 protein atoms, 189 solvent molecules and 44 NAD^+ atoms, while the overall *B*-factor is unusually high: 47 $Å^2$.**

The structure of LipDH Val reveals the conformation of the C-terminal residues which fold "back" into the putative lipoamide binding region. The C-terminus has been proven to be important for activity by site-directed mutagenesis. However, the distance of the C-terminus to the catalytically essential residues is surprisingly large, over 6 Å, and the precise role of the C-terminus still needs to be elucidated.

In this crystal form LipDH Val contains one NAD^+ molecule per subunit. Its adenine-ribose moiety occupies an analogous position as in the structure of glutathione reductase. However, the nicotinamide-ribose moiety is far removed from its expected position near the isoalloxazine ring and points into solution.

Comparison of LipDH Val with *Azotobacter vinelandii* lipoamide dehydrogenase yields an rms difference of 1.6 Å for 440 well defined C_α atoms per subunit. Comparing LipDH Val with glutathione reductase shows large differences in the tertiary and quaternary structure of the two enzymes. For instance, the two subunits in the dimer are shifted by 6 Å with respect to each other. So, LipDH Val confirms the surprising differences in molecular architecture between glutathione reductase and lipoamide dehydrogenase, which were already observed in *Azotobacter vinelandii* LipDH. This is the more remarkable since the active sites are located at the subunit interface and are virtually identical in all three enzymes.

Key words: X-ray crystallography, disulfide oxidoreductases, FAD, NAD^+, catalysis

INTRODUCTION

Lipoamide dehydrogenase (LipDH) is a ubiquitous FAD-dependent enzyme, which catalyzes the following reaction:

$$Lip(SH)_2 + NAD^+ \rightarrow LipS_2 + NADH + H^+.$$

LipDH belongs to the family of the disulfide oxidoreductases, which comprises also glutathione reductase, trypanothione reductase, mercuric reductase, thioredoxin reductase, and NADH peroxidase. In most of these enzymes the redox center is formed by the flavin ring together with a disulfide bridge and the catalyzed reaction proceeds via the formation of a charge transfer complex between the prosthetic group and one of the cysteine residues forming the SS bridge.[1] A specific feature of lipoamide dehydrogenase resides in its membership of several multienzyme complexes, like the pyruvate dehydrogenase complex and the branched chain oxoacid dehydrogenase complex. LipDH has, however, also been found in anaerobic organisms and a number of different metabolic functions have been attributed to the enzyme.[2] Quite remarkably in *Trypanosoma brucei* a lipoamide dehydrogenase occurs which is not part of a multienzyme complex and is possibly membrane associated.[3] Its ubiquitous distribution indeed suggests that LipDH could be one of the most ancient members of the disulfide oxidoreductases family.

Received August 12, 1991; accepted December 20, 1991.
Address reprint requests to Wim G. J. Hol, BIOSON Research Institute, Department of Chemistry, University of Groningen, Nijenborgh 16, 9747 AG Groningen, The Netherlands.

Abbreviations used: LipDH, lipoamide dehydrogenase; LipDH Val, lipoamide dehydrogenase occurring in the branched chain oxoacid dehydrogenase complex of *Pseudomonas putida;* rms, root mean square; PEG, polyethyleneglycol; HEPES, *N*-2-hydroxyethylpiperazine-*N'*-ethanesulfonic acid.

Lipoamide dehydrogenase is active as a dimer, usually of molecular weight of about 100,000,[1] the catalytic centers being located at the subunit interface. The structure of oxidized *Azotobacter vinelandii* LipDH has been solved and refined at 2.2 Å resolution[4,5] revealing a number of significant differences with respect to human glutathione reductase[6] in the tertiary and quaternary structure of the protein. Furthermore, in the crystal structure of *A. vinelandii* LipDH the 10 C-terminal residues appeared to be disordered, while mutagenesis experiments[7] clearly showed that these amino acids are essential for the enzymatic activity. In order to obtain more insight into the rather complex catalytic properties of LipDH, we have undertaken the structure determination of the complex between NAD$^+$ and LipDH Val that is one of the three different lipoamide dehydrogenases produced by *Pseudomonas putida*.[8] LipDH Val is strictly specific for the branched chain oxoacid dehydrogenase complex and its gene has been cloned and sequenced, indicating 42% sequence identity with *A. vinelandii* LipDH[9] (Fig. 1).

As expected, the three-dimensional structures of the two LipDH molecules are very similar, each subunit being composed of 4 domains, the FAD-binding domain, the NAD-binding domain, the central domain, and the interface domain (Fig. 2). In the present report, we shall focus on the new aspects revealed by the structure of LipDH Val (NAD$^+$-binding and conformation of the C-terminal residues), while for an overall description of the molecule we refer to the previous papers concerning *A. vinelandii* LipDH.[4,5]

MATERIALS AND METHODS

Crystals and Data Collection

LipDH Val was purified as described by Sokatch et al.[8] Immediately before crystallization the protein was loaded to a Mono Q HR 5/5 anion-exchange column on a Fast Protein Liquid Chromatography system (Pharmacia) and then eluted with a linear NaCl gradient (0.0–0.2 M) in Hepes buffer, pH 8.0. Fractions at 0.18–0.20 M were collected and used for crystallization experiments. This purification step greatly enhanced the quality of the crystals. Resolutions higher than 3.3 Å could be obtained only with the purified enzyme. Native electrophoresis gels suggest that ion-exchange chromatography was required to remove protein aggregates formed in solution. The crystals used for the structure determination were grown by the vapor diffusion method at 20°C. Five-microliter aliquots containing 10 mg protein/ml and 20 mM NAD$^+$ were added to 5–10 μl of 16% (w/v) PEG 6000 (Merck). Both solutions were buffered by 50 mM Hepes pH 7.0, 0.5 mM EDTA, 0.02% NaN_3. Hanging or sitting drops were equilibrated against 1 ml reservoir solution containing 15% PEG 6000. Crystals grew to a maximum size of $0.5 \times 0.4 \times 0.2$ mm in 1 week. They could be obtained also without the addition of NAD$^+$, but these crystals appeared to be of smaller size and less isometrically shaped. Zero layer precession photographs revealed space group $C222_1$ with cell dimensions $a = 62.3$ Å, $b = 108.1$ Å, and $c = 151.1$ Å. Assuming one subunit per asymmetric unit, this corresponds to a V_M of 2.40 Å^3/dalton and a solvent content of 47%, which is well within the usual range.[12]

X-Ray intensities were collected on the X31 beam line of the DESY synchrotron in Hamburg. Data were recorded by the oscillation method on a FUJI image plate detector at 20°C using a wavelength of about 1 Å. Two data sets (Table I) were collected with an oscillation range of 1° and 2°, respectively, while the crystal to detector distance was set to 280 and 403 mm in the two different experiments, the long distance allowing measurements of the low resolution data. The data sets were processed and merged together using the MOSCO program[13] yielding a total of 18,916 independent reflections. This corresponds to 97% of all possible reflections between 12.0 and 2.45 Å. The merging R-factor ($\Sigma (|I - \langle I \rangle|)/\Sigma I$) is 7.2% for 18731 reflections. It increases to 18.9% for the reflections in the highest resolution shell (2.50–2.45 Å).

Molecular Replacement

In order to solve the phase problem use was made of the homology with the known structure of lipoamide dehydrogenase from *A. vinelandii*.[4,5] The sequence identity between this protein and LipDH Val is 42%[9] (Fig. 1). By means of the molecular replacement method the orientation and position of the molecule in the crystal could be determined. The search model was subunit A of *A. vinelandii* LipDH.[5] The rotation function[14] was calculated with 3,000 reflections between 10.0 and 3.0 Å resolution. The inner and outer integration radius were set to 3.0 and 20.0 Å, respectively. A single peak 3σ above the mean was found and it corresponded to an orientation compatible with the molecular 2-fold axis being parallel to the crystallographic a axis.

For the the calculation of the translation function[15] data between 10.0 and 4.0 Å were employed. The translation indicated by the highest consistent peaks on the three Harker sections was applied to the model. This yielded an R-factor of 54%, which could be further reduced to 51% by 4 cycles of rigid-body refinement.[16] In this position the molecular 2-fold relating the subunits of the dimer coincides with the crystallographic twofold along the a axis.

Subsequently, the side chains of the rotated and translated search model were replaced according to the amino acid sequence of LipDH Val[9] by using the option "mutate" of the program Whatif.[17] This structure was the starting model for the crystallographic refinement.

```
           10        20        30                40        50
val QQTIQTTLLIIGGGPGGYVAAIRAGQLGIPTVLVEGQA-------LGGTCLNIGCIPSKALI
azo --SQKFDVIVIGAGPGGYVAAIKSAQLGLKTALIEKYKGKEGKTALGGTCLNVGCIPSKALL
              10        20        30        40        50        60
           eeeee hhhhhhhhhhhhhh  eeeee              hhhhhhhhhhhhhhh
             A1        1.1        A2                            1.2

       60        70        80        90       100       110
val HVAEQFHQASRFTEPSPLGISVASPRLDIGQSVAWKDGIVDRLTTGVAALLKKHGVKVVHGW
azo DSSYKFHEAHESF--KLHGISTGEVAIDVPTMIARKDQIVRNLTGGVASLIKANGVTLFEGH
           70        80        90       100       110       120
    hhhhhhhhhhhh                hhhhhhhhhhhhhhhhhhhhhhhh   eeeee e
                                          1.3                 A3

    120       130             140       150       160       170
val AKVLDGKQVEVDG-----QRIQCEHLLLATGSSSVELPMLPLGGPVI-SSTEALAPKALPQH
azo GKLLAGKKVEVTAADGSSQVLDTENVILASGSKPVEIPPAPVDQDVIVDSTGALDFQNVPGK
          130       140       150       160       170       180
    eeee    eeeee     eeeee  eeee eeeee              hhhhhh       e
     B1       B2        B3    A4    F1                 2.4

        180       190       200       210       220       230
val LVVVGGGYIGLELGIAYRKLGAQVSVVEARERILPTYDSELTAPVAESLKKLGIALHLGHSV
azo LGVIGAGVIGLELGSVWARLGAEVTVLEAMDKFLPAVDEQVAKEAQKILTKQGLKILLGARV
         190       200       210       220       230       240
    eeeee hhhhhhhhhhhhhhh eeeeee         hhhhhhhhhhhhhh  eeeee  ee
    C1         2.5          C2                2.6          C3

      240           250       260       270       280       290
val EGYEN----GCLLANDAKGGQLRLEA-DRVLVAVGRRPRTKGFNLECL-DLKMNGAAIAIDE
azo TGTEVKNKQVTVKFVDAEG--EKSQAFDKLIVAVGRRPVTTDLLAADSGVTLDERGFIYVDD
       250       260       270       280       290       300
    eeee     eeeeee      eeeee eeeeee eeeee
     D1       D2          D3    C4     F2

          300       310       320       330       340       350
val RCQTSMHNVWAIGDVAGEPMLAHRAMAQGEMVAEIIAGKARRFEPAAIAAVCFTDPEVVVVG
azo YCATSVPGVYAIGDVVRGAMLAHKASEEGVVVAERIAGHKAQMNYDLIPAVIYTHPEIAGVG
       310       320       330       340       350       360
     eee   eeeee         hhhhhhhhhhhhhhhhh              eeee   eeeeee
      A5     A6                 3.7                     E1      E2

        360       370       380       390       400       410
val KTPEQASQQGLDCIVAQFPFAANGRAMSLESKSGFVRVVARRDNHLILGWQAVGVAVSELST
azo KTEQALKAEGVAINVGVFPFAASGRAMAANDTAGFVKVIADAKTDRVLGVHVIGPSAAELVQ
      370       380       390       400       410       420
     hhhhh       eeeeeee             eeeeeee     eeeeeeeee hhhhhhh
      4.8           E3                  E4          E5

      420       430       440       450
val AFAQSLEMGACLEDVAGTIHAHPTLGEAVQEAALRALGHALHI-----
azo QGAIAMEFGTSAEDLGMMVFAHPALSEALHEAALAVSGHAIHVANRKK
   430       440       450       460       470
    hhhhhhh    hhhhhh        hhhhhhhhhh
      4.9      4.10            4.11
```

Fig. 1. Structure-based alignment of *A. vinelandii* LipDH and LipDH Val. Residues involved in α-helices and β-strands are indicated by the letters h and e, respectively. The nomenclature of the secondary structure elements is the same as used in refs. 5 and 10: each α-helix (h) is labeled by two digits, the first indicating the domain where the helix is located and the second giving its sequential number; each β-strand (e) is indicated by a letter giving the sheet name and a figure indicating its sequential number.

Refinement Method

For the crystallographic refinement the GROMOS molecular dynamics package adapted for X-ray crystallographic refinement by Fujinaga et al.[18] was used. Both energy minimization and molecular dynamics refinement algorithms were employed. For the latter the time step was set to 2 fsec, while the cutoff radius for the nonbonded distances was set to

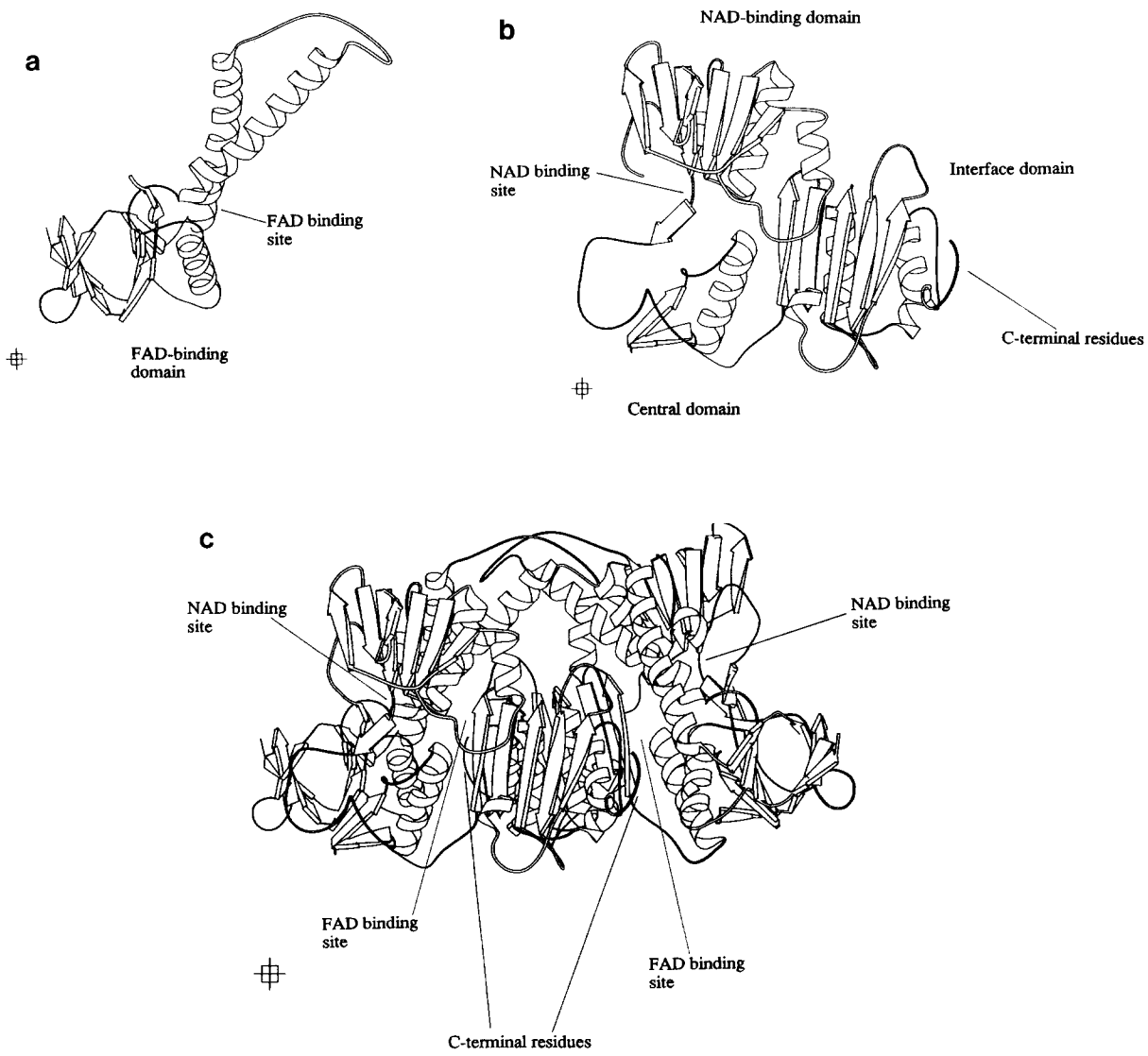

Fig. 2. Ribbon[11] diagrams of the structure of LipDH Val. **(a)** The FAD-binding domain. **(b)** The NAD-binding, the central and the interface domain. **(c)** The whole dimer. It has been generated by applying a 180° rotation about the molecular and crystallographic 2-fold axis, which runs vertically in the plane of the page. The direction of view is the same in **(a)**, **(b)**, and **(c)**.

5.0 Å. Throughout the refinement the contacts between symmetry related molecules were taken into account. The general principles of the protocol applied during the molecular dynamics refinement have been already described.[19] Essentially, it makes use of a weighting procedure for the X-ray term suited to allow large atomic shifts by overcoming high energy barriers. At the beginning of the simulation the weight applied to the X-ray gradients is low and then it is gradually increased in order to move the atoms toward positions which minimize the X-ray "pseudo energy-term." Initially also the resolution of reflections only extended to 4.0 Å, which was gradually increased to 2.4 Å (Table II). In this way even significant errors in the model can be automatically corrected.[19]

The *B*-factors were refined by the program TNT[16] which was also used in the latest stages to carry out conventional crystallographic refinement.

Peaks 3σ above the mean were searched in the $|F_o|-|F_c|$ map by the program Pekpik from the Xtal package.[20] Solvent molecules were assigned to each of them if they were at a distance shorter than 3.5 Å from at least one H-bond donor or acceptor. This procedure led to the location of 189 waters, whose average *B*-factor after refinement is 58 Å^2.

$2F_o-F_c$ σ_A weighted density maps[21] were calculated and manual model building was carried out on

TABLE I. Summary of the Data Collection

	High resolution	Low resolution	High + low
Wavelength (Å)	1.009	1.002	
Collimator (mm)	0.3×0.3	0.3×0.3	
Oscillation range (°)	1.0	2.0	
Resolution (Å)	2.45	3.8	
Refls. measured	80786	20210	100996
Refls. unique*	17505	5237	18916
R_{sym}†	6.4	6.4	7.2

*Number of unique reflections between 12.0 and 2.45 Å.
†$R_{sym} = \Sigma|I-\langle I\rangle|/\Sigma\langle I\rangle$.

an Evans & Sutherland Picture System 390, using the program FRODO.[22]

RESULTS

Course of the Refinement and Final Model

The whole refinement procedure consisted of 4 molecular dynamics runs followed by a few cycles of energy minimization alternated by manual model building (Table II). In the last stage the NAD^+ was modeled in the electron density and a further run of molecular dynamics refinement was carried out. The present model has a crystallographic *R*-factor of 21.8% for 18,216 observed unique reflections between 10.0 and 2.45 Å. It contains 458 residues, 189 solvent molecules, and the two cofactors NAD^+ and FAD. The rms difference between the starting and the final structure is 1.6 Å. The estimated coordinate error for 3,702 atom is 0.38 Å.[21] This model still presents one poorly defined region on the surface of the molecule (residues 248–253). In spite of many attempts, its conformation could never be adequately characterized. Not surprisingly this loop was also problematic in the structure determination of the *A. vinelandii* LipDH at 2.2 Å resolution.[5]

The root mean square differences from the ideal values of all the geometric parameters are in the range expected for this resolution (Table III). Most of the ϕ,ψ torsion angle combinations are in or very near the allowed regions,[24] 10 residues still having wrong combinations. These amino acids are listed in Table III. In Figure 3 the density of the C-terminal residues is shown. It gives an indication of the quality of the density for most of the atoms of the current model.

The average *B*-factor of all protein atoms obtained by the refinement procedure is 47 $Å^2$ (Table III), higher than values normally found in proteins. Exactly the same value is indicated by a Wilson plot calculated with all the reflections used in the refinement. The *B*-factors are quite uniformly distributed over the entire molecule (Fig. 4), although residues 160–240 of the NAD-binding domain have no regions with high *B*-factors. This suggests that this unusually high degree of mobility is most likely due to static disorder and not to the presence of very flexible protein regions. This observation might be related to the low occupancy of NAD^+. The partial occupancy of its binding site, situated in a region of crystal contacts, could cause disorder in the packing interactions between molecules in the crystal. Poor convergence during crystallographic refinement associated with high average temperature factor has been observed in the crystal structure of the ternary complex folate–NADP–*E. coli* dihydrofolate reductase.[25] In our case convergence was not a serious problem.

The Overall Structure

The overall structure of LipDH Val (Fig. 2) is, as expected, very similar to the structure of *A. vinelandii* LipDH. The rms difference between all 440 equivalent C_α atoms of the two structures is 1.60 Å, with most of the main variations being localized at the surface of the molecule. After removing the surface residues deviating more than 4 Å, the rms difference drops to 1.1 Å for 363 equivalent residues, falling into the range of values expected for 42% sequence identity.[26] Based on the structural comparison LipDH Val shows 3 insertions with respect to *A. vinelandii* LipDH. These are residues 1–2, 68–69 and 251–252 (Fig. 1). Moreover there are 6 deletions, occurring between residues 38–39, 130–131, 159–160, 241–242, 256–257 and 278–279. The degree of homology between the two proteins does not differ significantly in the 4 domains ranging from 40 to 44%. However, the amino acid changes are not equally distributed along the polypeptide chain. The 11 α-helical regions and the 23 β-strands have sequence identities of 57 and 54%, respectively, while in the other parts of the molecule this value drops to 29%.

The four domains forming each subunit, the FAD-binding domain, the NAD-binding domain, the central domain, and the interface domain, comprise residues 1–142, 143–268, 269–337 and 338–458, respectively (Fig. 2). Their topology as well as the topological identity between the NAD-binding and FAD-binding domains[27] has already been extensively described.[5,10] The secondary structure elements of LipDH Val are indicated in Figure 1. The two subunits forming the dimer are related by the crystallographic 2-fold along the *a* axis. Upon dimerization 3650 $Å^2$ of the solvent accessible surface (calculated with the program DSSP written by Kabsch and Sander[23]) becomes buried. This value is higher than that observed in *A. vinelandii* LipDH[5] (2,700 $Å^2$) and in glutathione reductase[6] (3,300 $Å^2$). This is partially accounted for by the involvement in the intersubunit interactions of the C-terminal residues, which could not be defined in *A. vinelandii* LipDH.

Our description of the LipDH Val molecule will mainly focus on the structural features newly re-

TABLE II. Course of the Refinement

Type of refinement	Resolution (Å)	*R*-factor* (%)	σ_B† (Å)	Number‡ of residues	*B*-factor	Number of waters
TNT	10.–4.00	42.9	0.033	450	overall	0
TNT	10.–3.20	42.0	0.028	450	overall	0
MD	10.–2.45	29.4	0.023	450	atomic	0
MD	10.–2.45	29.5	0.016	440	atomic	0
MD	10.–2.45	26.8	0.023	445	atomic	0
MD	10.–2.45	25.6	0.022	456	atomic	0
TNT	10.–2.45	23.5	0.018	456	atomic	130
MD	10.–2.45	21.8	0.022	458	atomic	189+NAD$^+$

*R-factor is defined as $R = \Sigma|F_o - F_c|/\Sigma|F_o|$.
†rms deviation from ideal values of the bonds as calculated by the program TNT.[16]
‡Number of residues included in the refinement.

TABLE III. The Geometry of the Final Model

Bonds*	(Å)	0.022
Angles*	(°)	4.2
Trigonal*	(Å)	0.005
Planar*	(Å)	0.030
Nonbonded*	(Å)	0.048
⟨*B*⟩	(Å)	47.0
Number of H-bonds/100 residues†		71
Number of wrong ϕ,ψ values‡		10

*rms difference from the ideal values. They were calculated by the program TNT.[16]
†Number of main chain H-bonds per 100 residues, calculated by the program DSSP.[23]
‡The following residues have wrong ϕ,ψ values: Gln-37, Gln-131, Glu-136, Leu-152, Asn-240, Gln-252, Asn-274, His-298, Glu-309, Ser-386. None of these residues occurs in secondary structure elements (Fig. 1) and all, except from Asn-274, His-298, and Glu-309, have *B*-factors which are considerably higher than average (Fig. 4).

vealed by this investigation. Particularly, the present structure allows an accurate description of the last 6 residues of the polypeptide chain. They were not visible in the *A. vinelandii* Lip DH structure, while mutagenesis experiments[7] have shown that these residues are essential for the normal activity of the enzyme. Moreover, the crystal structure of LipDH Val shows NAD$^+$ to be bound in an unexpected conformation, although with low occupancy.

Conformation of the C-Terminal Residues

In the structure of *A. vinelandii* LipDH[5] the last 10 amino acids (residues 466–476) of the polypeptide chain were not visible in the density. On the other hand, the results obtained by Benen et al.[7] clearly pointed toward an essential role for these residues, since deletion mutants of *A. vinelandii* LipDH lacking the last 9 or 14 amino acids were not active. Furthermore, all known LipDH sequences[1,4,28] contain this C-terminal extension, which is not present in glutathione reductase.[29] It was therefore of great interest to see whether the structure of LipDH Val could provide more information about this region. With respect to the sequence of *A. vinelandii* LipDH, LipDH Val has the C-terminal arm shortened by 5 residues,[9] since its last amino acid (Ile-458) corresponds to residue 471 of *A. vinelandii* LipDH (Fig. 1).

Already the $2F_o - F_c$ map calculated with the model after molecular replacement indicated that the C-terminal part was visible in the electron density map. It is worth mentioning that, since this part of the molecule was not present in the search model, its density was completely unbiased. A first run of molecular dynamics refinement still omitting these amino acids further clarified the density map and, after that, the backbone atoms together with the side chains could be unambiguously located. A final $2F_o - F_c$ omit map for residues 453–458 is shown in Figure 3. Their average *B*-factor is 31.2 Å^2.

The C_α tracing of LipDH Val together with the position of its C-terminal residues is schematically shown in Figure 2. As can be seen, the last 5 amino acids form an arm protruding into the putative lipoamide binding site (si face of the flavin ring) at the interface between the two subunits. The H-bonds formed by these residues are depicted on Figure 5. One of these (O Ala-455–NE2 Gln 26′) involves an amino acid of the opposite subunit. Furthermore, 13 atoms are within 4.0 Å distance from atoms of the other monomer (Table IV). Upon dimerization 307 Å^2 of the accessible surface of these residues become buried by interacting with the C-terminal residues.

The deletion mutants of *A. vinelandii* LipDH lacking the last 9 or 14 residues are not active with the physiological substrate NAD$^+$, due to product inhibition. Upon formation of NADH the enzyme is rapidly overreduced (i.e., the $FADH_2$·SHSH form is generated) and becomes inactive, possibly indicating an increase in the redox potential of the flavin.[7] Similar changes in the properties of the enzyme (product inhibition and overreduction) were also observed with a mutant of *A. vinelandii* LipDH, where a Tyr residue (equivalent to Tyr-18 in LipDH Val; Fig. 5) was replaced by Phe. The structure of LipDH

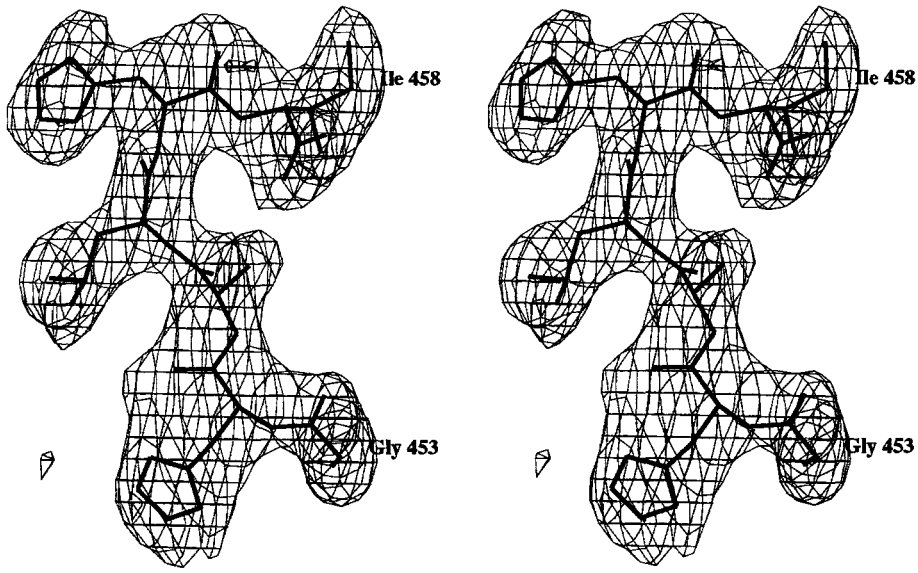

Fig. 3. Stereo picture of the $2F_o-F_c$ map for the C-terminal residues 453–458. The contour level is 1σ. These amino acids were omitted in the calculation of the electron density. The *R*-factor with these residues omitted was 23%.

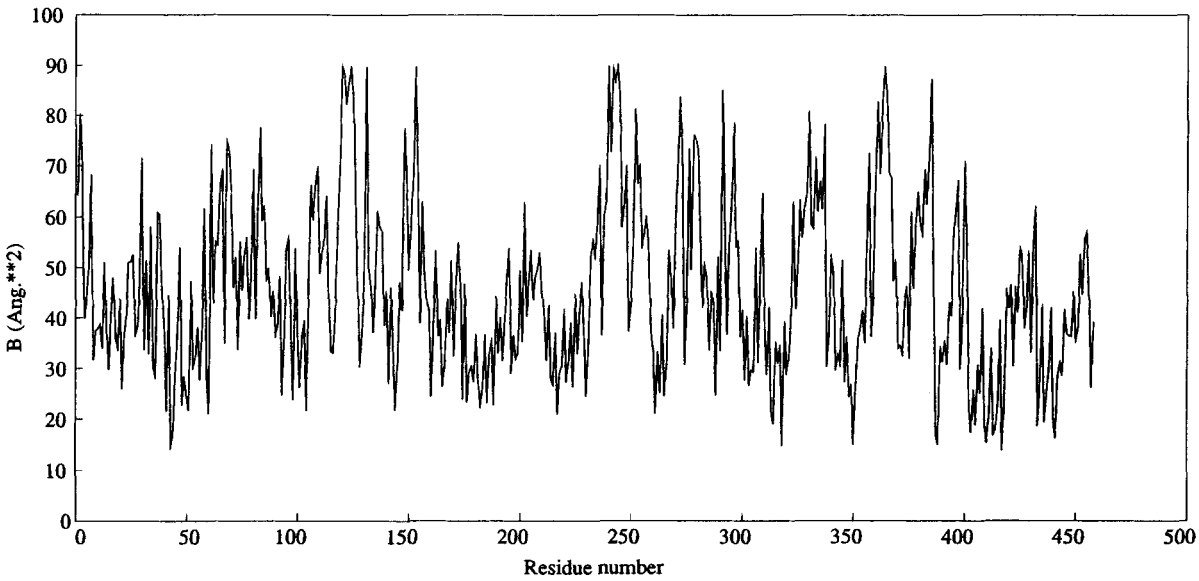

Fig. 4. Plot of the averaged per residue *B*-factors of the main chain atoms.

Val shows that this amino acid is weakly interacting with His-457 of the opposite subunit (Fig. 5). A Tyr side chain this position is conserved in all known LipDH sequences.[1,4]

The C-terminal residue nearest to the reactive disulfide bridge is His-457, which is more than 8 Å away from the distal cysteine (Cys-43 on the opposite chain). Also the hydroxyl group of Tyr-18 is very far (6.1 Å; see Fig. 5) from the catalytic disulfide bridge. These observations raise the question of how these side chains can exercise a long-range effect on the catalytic and possibly redox properties of the enzyme. We do not have an explanation for this fact. The opening of the lipoamide binding site upon removal of the C-terminal residues could make the flavin environment more solvent accessible and therefore more polar. This could have an influence on the cofactor, possibly increasing its redox potential. Obviously, the conformation of the C-terminus could be significantly altered upon lipoamide bind-

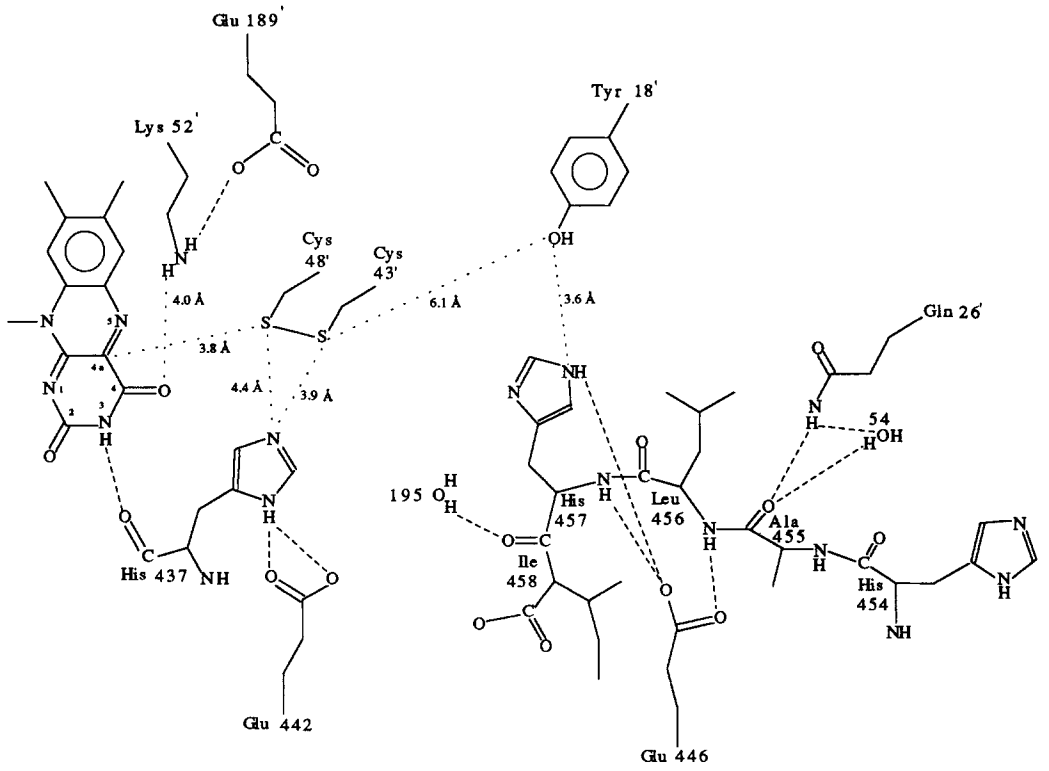

Fig. 5. Schematic picture of the interactions made by the C-terminal residues on the *si* side of the flavin. Amino acids of the opposite subunit are indicated by a prime symbol following their sequence number. H-bonds ($d < 3.4$ Å) are shown by dashed lines, while the dotted lines indicate distances between residues directly or indirectly involved in catalysis.

ing and we are currently undertaking the structure determination of *Pseudomonas fluorescens* LipDH of which crystals have been grown in the presence of 10 mM of lipoamide.

NAD^+ Binding

The electron acceptor in the physiological reaction catalyzed by LipDH is NAD^+, which binds on the re side of the flavin ring. The crystallographic studies on glutathione reductase[30,31] have shown that the nicotinamide ring of NADPH sits parallel to the middle ring of the flavin, strongly supporting the model of hydride transfer between the prosthetic group and NADPH. Furthermore, to allow the binding of the substrate, the side chain of a tyrosine (Tyr-197) has to swing out of the nicotinamide binding site. This residue is replaced by Ile or Val, in virtually all LipDH sequences known at present,[1] the only exception to this rule being the sequence of LipDH Val, where a tyrosine side chain (Tyr-181; Fig. 1) is conserved.

The crystals of LipDH Val could be grown either with or without the addition of NAD^+. However, the presence of 10 mM substrate improved their quality, since they appeared to be of slightly bigger size and better shape. Analysis of precession pictures indicated that the crystals of the enzyme–substrate complex were isomorphous to the native ones. A strong peak in the position expected to be occupied by the pyrophosphate moiety of NAD^+ could already be observed in the electron density map calculated with the model after rigid body refinement. Furthermore, after additional refinement steps, two other electron density peaks could be ascribed to the adenine and nicotinamide rings. However, only weak density could be found for one of the ribose groups and in the final map (Fig. 6) a gap between the nicotinamide ribose and the pyrophosphate is still present. The weakness of the electron density suggests that the substrate is bound with low occupancy or not in a unique conformation or both. The average *B*-factor for 44 NAD^+ atoms is 68 $Å^2$, higher than the average value found for the protein atoms. The NAD^+ binding site is located in a region of contacts between two molecules related by the crystallographic 2-fold parallel to the *b* axis, although NAD^+ is not in direct contact with a neighboring LipDH molecule. As already discussed, the unusually high value of the protein average *B*-factor (Table III) could be due to the disorder and/or low occupancy of NAD^+. This might be a consequence of inhomogeneity in the molecular packing inside the crystals. However, crystals grown in the absence of NAD^+ do not diffract better, which indicates that other reasons

TABLE IV. Interactions of the Last 5 Residues of LipDH Val With Other Protein Atoms*

Residue	Atom of the C-terminal residue	Protein atom in contact†		Distance (Å)	
His-454	N	C	Leu-449	3.9	
	N	O	Leu-449	2.9	HB‡
	C_α	O	Leu-449	3.8	
	C	O	Leu-449	3.8	
	O	C_β	Leu-449	3.7	
	O	$C_\delta 2$	Leu-449	3.8	
	C_β	C_ζ	Arg-23′	3.5	
	C_β	$N_\eta 1$	Arg-23′	3.2	
	C_γ	$N_\zeta 1$	Arg-23′	3.8	
	C_γ	$N_\eta 1$	Arg-23′	3.8	
	C_γ	$N_\eta 2$	Arg-23′	3.7	
	$N_\delta 1$	$C_\delta 2$	Leu-449	3.5	
	$N_\delta 1$	C_ζ	Arg-23′	3.9	
	$N_\delta 1$	$N_\eta 2$	Arg-23′	3.7	
	$C_\epsilon 1$	$C_\delta 2$	Leu-449	3.5	
Ala-455	C_α	C_β	Leu-449	3.8	
	C_β	$O_\epsilon 2$	Glu-446	3.8	
	C_β	N	Arg-450	3.9	
	C	$N_\epsilon 2$	Gln-26′	3.7	
	O	C_δ	Gln-26′	3.5	
	O	$N_\epsilon 2$	Gln-26′	2.6	HB
Leu-456	N	$O_\epsilon 1$	Glu-446	3.2	HB
	C_α	$O_\epsilon 1$	Glu-446	3.9	
	$C_\delta 2$	C_γ	Arg-23′	3.5	
	O	$C_\delta 1$	Ile-22′	3.6	
	O	$C_\delta 1$	Ile-105′	3.4	
	O	$C_\delta 2$	Ile-105′	3.7	
His-457	N	C_δ	Glu-446	3.8	
	N	$O_\epsilon 1$	Glu-446	3.6	
	N	$O_\epsilon 2$	Glu-446	3.4	HB
	C_α	$C_\delta 1$	Leu-105′	3.8	
	C	$C_\delta 1$	Leu-105′	3.9	
	O	C_β	Ala-375	3.8	
	C_γ	$O_\epsilon 1$	Glu-446	3.6	
	$N_\delta 1$	$O_\epsilon 2$	Glu-446	2.8	HB
	$C_\epsilon 1$	$O_\epsilon 2$	Glu-446	3.9	
	$C_\epsilon 1$	$C_\gamma 2$	Val-19′	3.9	
	$N_\epsilon 2$	$C_\epsilon 2$	Tyr-18′	3.8	
	$N_\epsilon 2$	O_η	Tyr-18′	3.8	
Ile-458	N	$C_\delta 2$	Leu-105′	3.9	
	C_β	$C_\epsilon 2$	Phe-371	3.7	
	$C_\gamma 2$	C_ζ	Arg-450	3.8	
	$C_\gamma 2$	$N_\eta 2$	Arg-450	3.6	
	$C_\gamma 1$	$N_\eta 2$	Arg-450	3.9	
	C	$C_\delta 2$	Leu-105′	3.7	

*All protein atoms being within 4.0 Å distance from residues 454–458 of LipDH Val are indicated. For sake of brevity, the interactions with residue 453 and those between atoms of the C-terminal amino acids are excluded from the analysis.
†The prime symbol indicates residues of the 2-fold related subunit.
‡HB identifies the H-bonded atoms.

might be the underlying cause of the high temperature factor in LipDH Val crystals.

The NAD^+ molecule is bound in a conformation such that an electron transfer between the substrate and the flavin could not take place since the nicotinamide ring sits outside of its expected binding site and points toward the solvent (Fig. 7). This situation is partially similar to that observed in glutathione reductase,[31] where the crystals soaked with $NADP^+$ indicated weak or no density for the NMN half of the molecule. That study also showed that $NADP^+$ was unable to promote the movement of the tyrosine side chain (Tyr-197), necessary to allow the nicotinamide to bind in the conformation required for the hydride transfer. The same observation holds (Fig. 7) for LipDH Val, where the binding of NAD^+ does not cause the swinging out of the aromatic side chain (Tyr-181). However, near this tyrosine, there are also two weak extra density peaks, which could indicate that part of the NAD^+ molecules may have their nicotinamide ring near the flavin. Attempts to model and refine the substrate in the two different conformations failed in clarifying these features in the density. Therefore, only the NAD^+ bound with the nicotinamide ring in the "out" conformation was modeled in the electron density and we shall focus only on the description of this conformation.

The NAD^+ atoms form 10 H-bonds with the protein (Fig. 8, Table V). They involve the adenine and the nicotinamide rings together with their ribose groups but not the pyrophosphate moiety, which does not show any interaction shorter than 3.5 Å with the protein.

Adenine and adenine ribose binding

The adenine ring is in the *anti* conformation, with a torsion angle about the glycosidic bond of 153°, very near to values found in mono- or dinucleotides.[32] It makes two H-bonds (Fig. 8) with backbone atoms, in an identical manner as the adenine ring of FAD. Indeed, the residues involved in the H-bonds (Ala-118 for the FAD adenine and Val-235 for the NAD^+ adenine) are topologically equivalent, being at the beginning of the first strand of the β-meander in the NAD- and FAD-binding domains.[27] Therefore, the very weak sequence homology between the two domains does not prevent the identity of some interactions between the adenine rings and the protein. This is further supported by the H-bonds between the ribose hydroxyl groups and a glutamate side chain, present in the binding of both FAD and NAD^+ (Glu-35 and Glu-201, respectively). Conservation of identical H-bonds among proteins with very weak sequence homology has been observed in the NAD^+ binding of different dehydrogenases[33] as well as in the FMN binding of glycolate oxidase and trimethylamine dehydrogenase.[34]

Two water molecules are at 4 Å distance from the adenine ring, which fits into a cleft surrounded by

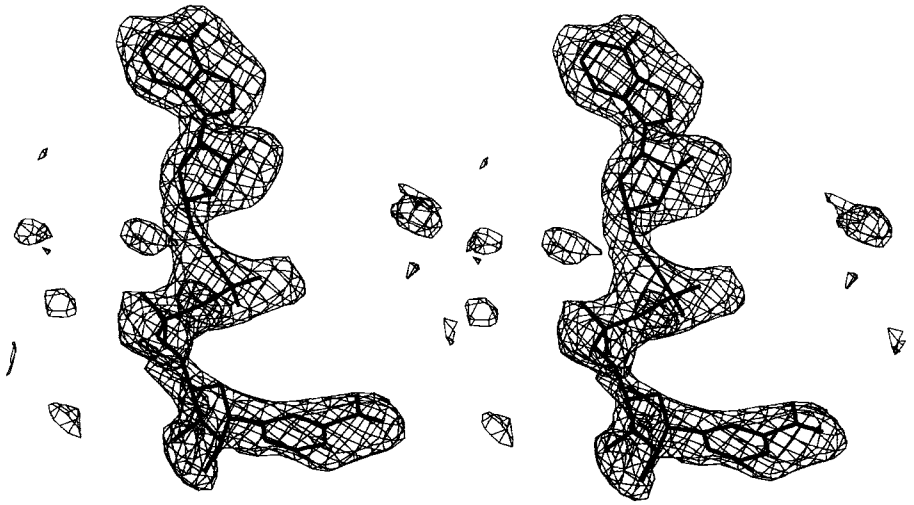

Fig. 6. Stereo picture of the $2F_o-F_c$ map for NAD$^+$. The contour level is 0.8σ. The atoms of the dinucleotide were omitted in the calculation of the electron density, otherwise the coordinates of the final model were used for the calculation of the structure factors.

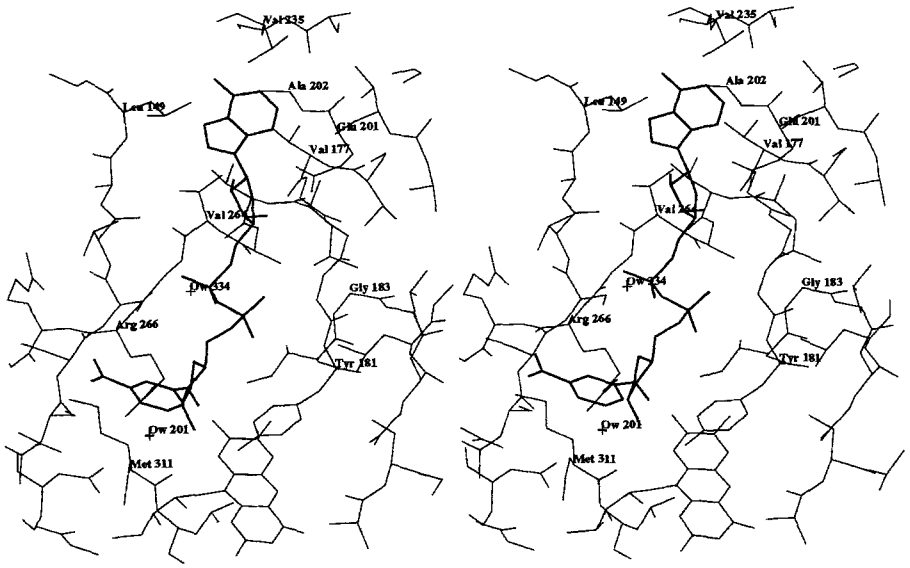

Fig. 7. Stereo representation of the atoms surrounding the NAD$^+$. For a more schematic description of the interactions involving the dinucleotide substrate see Figure 8.

the side chains of Val-177, Ala-202, Ser-234, and Val-264 (Fig. 7). The hydrophobic character of these residues is conserved among all known LipDH sequences,[1] with the exception of Ser-234, which can be replaced by Lys or Arg. Their aliphatic parts can, however, also provide a hydrophobic environment.

The conformation of the adenine ribose has been modeled as C2′ *endo*, in agreement with that observed in mono and dinucleotides with the adenine in the *anti* conformation.[32]

Recently, Scrutton et al.[35] have changed by site-directed mutagenesis the substrate specificity of *E. coli* glutathione reductase, which has been transformed from an NADPH-dependent into an NADH-dependent enzyme. One of the most striking results in their beautiful work was that the substitution in the α-helix of the βαβ fold of an Ala residue (corresponding to Gly 183 of LipDH Val) by Gly can by itself cause a significant drop in the K_m for NADH. An alanine in this position is indeed characteristic (but not absolutely required) of the NADPH binding fold, while the NADH binding proteins in this location have a Gly.[36]

The superposition of the NAD-binding βαβ region

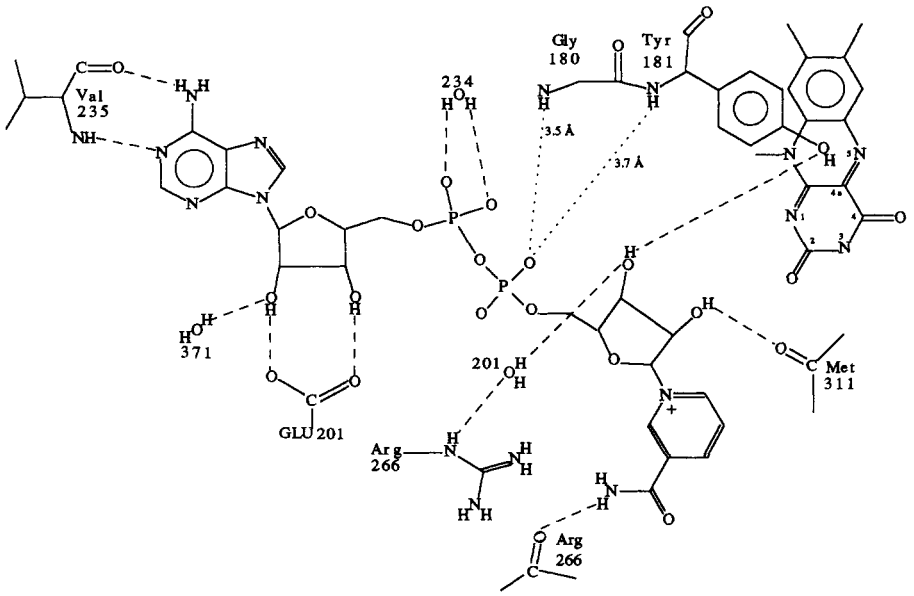

Fig. 8. Schematic drawing of the H-bonds ($d < 3.4$ Å) involving NAD^+ atoms. They are indicated by the dashed lines. The dotted lines illustrate the interactions between the pyrophosphate oxygens and the residues at the N-terminus of the α-helix beginning at residue 180.

of LipDH Val (residues 175–208) onto the homologous part of glutathione reductase (residues 191–224[6]) yields a sequence identity of 33% and gives an rms difference of 0.87 Å for 34 C_α atoms, the most significant shift occurring (Fig. 9) at position 179 (1.6 Å). The latter movement is also observed in the structure of *A. vinelandii* LipDH[5] (data not shown). This shift of Gly-179 is most likely due to the Ala–Gly difference at position 183: in LipDH the C_β methyl group would come too close to the main chain atoms of Gly-179. This is illustrated in Figure 9 by the hypothetical 2.3 Å distance between C_β of Ala-183 in glutathione reductase and the carbonyl oxygen of residue 178 in LipDH Val. As a consequence, Gly-179 moves further away from residue 183 in glutathione reductase than in LipDH. The motion of Gly-179 occurs very near Glu-201 of LipDH, which is H-bonded to the backbone nitrogen of Gly-179 and to both the 2′ and 3′ hydroxyl of the adenine ribose. It is important to realize that in glutathione reductase the negative charge of Glu-201 is approximatively replaced by the 2′-phosphate of NADP, which is interacting with the positive charges Arg-218 and Arg-224.[31] Hence fine tuning of the NADP/NAD preference of βαβ folding units can occur in an indirect manner, via Gly-179 by the addition/removal of a single methyl group at position 183.

Pyrophosphate binding

The adenine phosphate does not make any strong H-bond with the polypeptide atoms but is H-bonded to a water molecule (Fig. 7 and Table V). A lack of direct interactions with the protein is also observed for the nicotinamide phosphate, because the curling out of the nicotinamide ring causes a loosening of the interactions between the phosphate oxygens and the backbone atoms of the α-helix of the βαβ fold, which starts at residue 180 (Fig. 8). The pyrophosphate is, however, still located near the N-terminus of this α-helix, allowing a favorable charge–helix dipole interaction.

Nicotinamide and nicotinamide ribose binding

The nicotinamide ribose has weak density (Fig. 6). Its conformation has been tentatively modeled as C3′ *endo,* with the hydroxyl groups forming three H-bonds (Fig. 8). They involve the side chain of Tyr-181, the carbonyl oxygen of Met-311, and a water molecule (Ow-201), which is in turn H-bonded to Arg-266. This network of interactions could be essential to keep the NAD^+ in the observed conformation. However, great caution is necessary in the interpretation of the present model, in view of the weakness of the ribose density.

The nicotinamide ring points toward the solvent and is bound in the *syn* conformation. The nitrogen of the carboxamide group interacts with the main chain oxygen of Arg-266, while the side chain of Met-311 (Fig. 7) is in contact with the aromatic ring.

One of the most interesting points raised by the structure determination of LipDH Val is why NAD^+ does not directly interact with the flavin. The positive charge is probably the most important factor in preventing the binding of the oxidized nicotinamide to its expected binding site. In the reduced state of the enzyme the negative charge due to the charge transfer complex is located in proximity of the flavin

TABLE V. Interactions* Between NAD$^+$ and Protein Atoms of LipDH Val

NAD$^+$ atom	Residue number	Residue name	Interacting atoms‡	H-bond§ Atom	H-bond§ d (Å)
NIA	177	Val	Side		
	233	His	Main		
	234	Ser	Main		
	235	Val	Side + main	N	3.0
C2A	177	Val	Side		
	200	Val	Main		
	202	Ala	Main		
	233	His	Main		
	235	Val	Main		
N3A	178	Gly	Main		
	200	Val	Main		
	201	Glu	Main		
	202	Ala	Side + main		
C4A	202	Ala	Side		
	264	Val	Side		
C6A	234	Ser	Main		
	235	Val	Main		
N6A	234	Ser	Side + main		
	235	Val	Main	O	3.4
C1'A	201	Glu	Side		
C2'A	201	Glu	Side		
O2'A	201	Glu	Side	OE1	3.2
	371	Sol		O	3.3
C3'A	201	Glu	Side		
O3'A	201	Glu	Side	OE2	3.2
	208	Pro	Side		
C4'A	178	Gly	Main		
	179	Gly	Main		
	201	Glu	Side		
	263	Ala	Main		
01'A	178	Gly	Main		
	179	Gly	Main		
	201	Glu	Side		
	264	Val	Main		
C5'A	263	Ala	Main		
	264	Val	Main		
PA	265	Gly	Main		
O1PA	234	Sol		O	2.4
O2PA	264	Val	Main		
	265	Gly	Main		
	234	Sol		O	2.9
O3P	265	Gly	Main		
PN	263	Ala	Main		
O1PN	180	Gly	Main		
	263	Ala	Main		

(continued)

TABLE V. Interactions* Between NAD$^+$ and Protein Atoms of LipDH Val (Continued)

NAD$^+$ atom†	Residue number	Residue name	Interacting atoms‡	H-bond§ Atom	H-bond§ d (Å)
O2PN	180	Gly	Main		
	181	Tyr	Side + main		
O5'A	182	Ile	Side		
	263	Ala	Main		
C5'N	182	Ile	Main		
	265	Gly	Main		
	266	Arg	Side		
C4'N	181	Tyr	Side		
	182	Ile	Side		
C3'N	182	Ile	Side		
	266	Arg	Side		
	201	Sol			
O3'N	181	Tyr	Side	OH	3.2
	182	Ile	Side		
	266	Arg	Side		
	459	FMN	Side		
	459	FMN	Flavin ring		
	201	Sol		O	3.0
C2'N	181	Tyr	Side		
	311	Met	Side + main		
	201	Sol			
O2'N	181	Tyr	Side		
	311	Met	Side + main	O	2.6
	201	Sol			
C1'N	181	Tyr	Side		
NIN	311	Met	Side		
C2N	311	Met	Side		
C2N	309	Glu	Main		
	311	Met	Side + main		
C4N	309	Glu	Main		
	310	Pro	Main		
	311	Met	Main		
C5N	310	Pro	Main		
	311	Met	Main		
C7N	309	Glu	Main		
	311	Met	Side		
O7N	266	Arg	Side		
	311	Met	Side		
N7N	266	Arg	Main	O	2.7

*Only NAD$^+$ atoms being at a distance less than 4.0 Å from a protein atom are indicated.

‡"Main" and "Side" indicate whether main chain atoms or side chain atoms or both interact with NAD$^+$. We have refrained from specifically listing individual atoms because of the uncertainty in the position of NAD$^+$ atoms as reflected by their high average temperature factors (68 Å^2).

§The atoms H-bonded (d<3.4 Å) to NAD$^+$ are indicated.

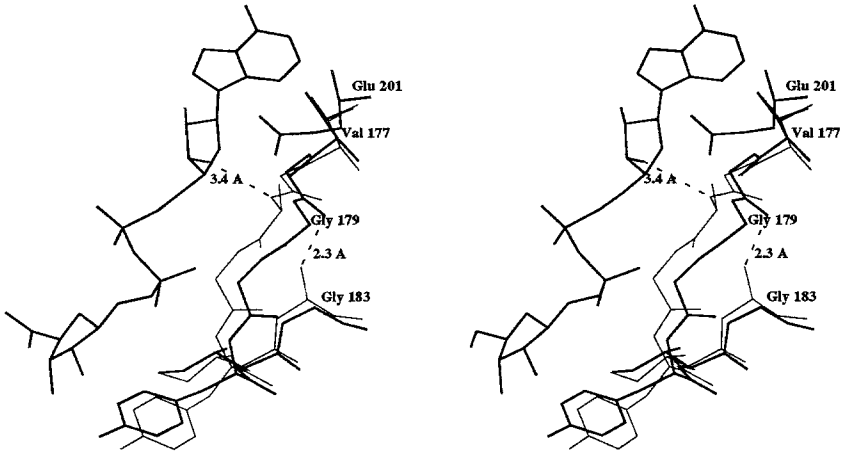

Fig. 9. The conformation of the glycine-rich loop involved in NAD(P) binding in glutathione reductase (thin line) and LipDH Val (thick line). The glutathione reductase coordinates are those of Karplus and Schulz [6] (PDB entry 3GRS). No coordinates of the glutathione reductase:$NADP^+$ complex are available, but the conformational changes induced by the substrate binding are small according to ref.[37] Also the NAD^+ conformation observed in LipDH Val is shown. The picture was obtained by superimposing residues 175–208 of LipDH Val and 191–224 of glutathione reductase, which gave an rms deviation of 0.87 Å for 34 atoms. The labels refer to LipDH Val numbering.

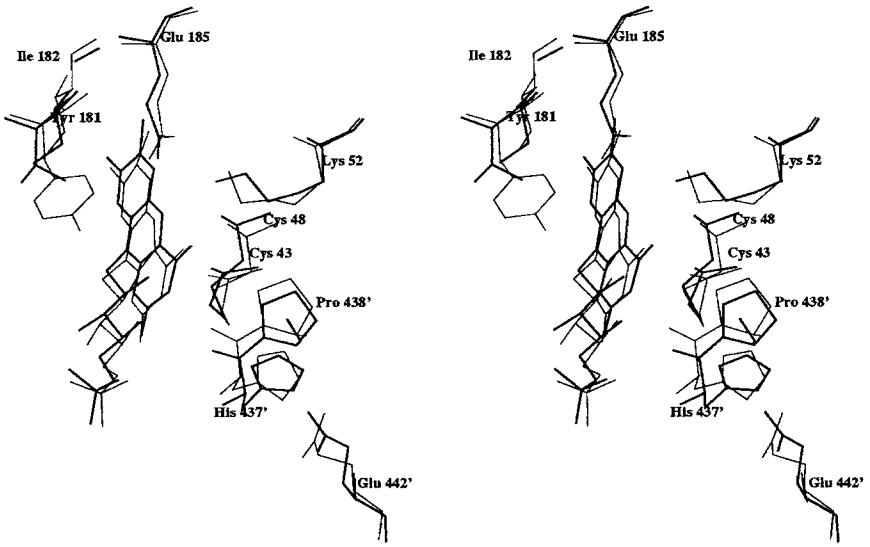

Fig. 10. Superposition of the catalytic centers in *A. vinelandii* LipDH (thin lines) and LipDH Val (thick lines). The picture was obtained by superimposing the *entire* A subunits of the two enzymes. Primed numbers indicate amino acids of the "opposite" subunit.

ring. It could therefore balance the opposite charge of NAD^+, making possible the interactions required for the hydride transfer between the prosthetic group and the substrate. In the oxidized state, as in the current study, the flavin would be neutral, and, therefore, not have a significant favorable electrostatic interaction with the positively charged nicotinamide ring of NAD^+. From this point of view, the structure of LipDH Val further substantiates the model of a ping-pong mechanism for the catalyzed reaction.[1] While the adenine part of NAD^+ binds independently from the redox state of the flavin, the nicotinamide can enter its binding site only upon reduction of the prosthetic group. This provides a nice electrostatic and structural basis for the discrimination between a sequential and a ping-pong mechanism.

The conformation of tyrosine-181

The side chain of Tyr-181 points toward the flavin ring (Fig. 7), in an identical way as in glutathione reductase. Indeed, the conformation of the side chain

is very similar in the two enzymes, with a χ_1 torsion angle of 90° in glutathione reductase[31] and 100° in LipDH Val (Fig. 9). This energetically unfavorable conformation could play a role in facilitating the movement required for nicotinamide binding.

There have been many speculations about a possible functional or structural role for this amino acid. An analogous tyrosine has been observed in ferrodoxin-NADP$^+$ reductase.[38] A mutant of *E. coli* glutathione reductase having the tyrosine replaced by serine presents a switch from the ping-pong to a sequential mechanism.[39] Furthermore, *E. coli* LipDH has been mutated by introducing a tyrosine in the same position as observed in glutathione reductase.[40] The comparison of the structure of LipDH Val with that of *A. vinelandii* LipDH gives the opportunity to check whether the presence of an aromatic side chain (LipDH Val) at position 181 instead of a branched side chain (*A. vinelandii* LipDH) causes any structural perturbation. Figure 10 clearly shows that this is not the case. The rms deviation after optimal superposition is 0.4 Å for 30 equivalent atoms. This analysis suggests that, at least in lipoamide dehydrogenase, the substitution of an aromatic with a branched side chain at position 181 does not cause significant changes in structure and in function of the enzyme. The question about the specific role, if any, played by the side chain of residue 181, seems to rely on further mutagenesis experiments, for instance when smaller side chains are introduced.

FAD Binding and Catalytic Center

The prosthetic group and the residues involved in catalysis are the least mobile regions of the protein with an average *B*-factor of 22.3 and 22.5 Å^2, respectively.

The binding and the conformation of FAD are very similar to that observed in *A. vinelandii* LipDH (Fig. 10). All 53 FAD nonhydrogen FAD atoms superimpose with an rms difference of 0.42 Å. The interactions between FAD and protein atoms are virtually the same, the only significant difference being the adenine ribose, which in LipDH Val is more solvent exposed. This is due to the absence between Gln-38 and Ala-39 of a 7 residues loop (Fig. 1), which in *A. vinelandii* LipDH partially covers the sugar moiety. The greater accessibility of the adenine ribose possibly reflects the higher temperature factor of the adenine (29 Å^2) with respect to the flavin part. Such a difference in thermal parameters is not observed in *A. vinelandii* LipDH.[5]

A high level of structural similarity also characterizes the catalytic centers. The differences in the atomic positions of the groups involved in catalysis are of the same order as the coordinate error (Fig. 10). In fact, neither the replacement of a Val side chain with tyrosine (Tyr-181) on the *re* side of the flavin nor the proximity of the ordered C-terminal residues on the *si* face causes significant conformational changes, when comparing the *P. putida* and *A. vinelandii* enzymes.

Comparison Between Lipoamide Dehydrogenase and Glutathione Reductase

The analysis of the structure of *A. vinelandii* LipDH revealed a number of significant differences with respect to glutathione reductase[6] both in the tertiary and quaternary structures of the enzyme.[5] This observation was of particular interest since the catalytic center is located at the subunit interface. When the FAD-binding domain was taken as a reference frame in the *A. vinelandii* LipDH versus glutathione reductase comparison, it appeared that the NAD binding and the interface domains were differently oriented by 7° and 8°, respectively. Moreover, the interface domain presented an additional distortion, due to different orientations of the individual α-helices. Finally, at the level of the quaternary structure, the dimer of LipDH appeared to be differently assembled. A 5 Å shift was detected by comparing the mutual position of the two subunits in *A. vinelandii* LipDH and in glutathione reductase.

The structure of LipDH Val essentially confirms these observations. No significant differences between the structure of *A. vinelandii* LipDH and LipDH Val are observed. After optimal superposition[41] of the secondary structure elements of the entire subunit (Fig. 1), the rms difference between 241 equivalent C_α atoms is 1.0 Å. This value does not change when individual domains are superimposed, the rms differences then ranging from 0.97 to 1.10 Å per domain. Therefore, the mutual arrangement of domains is essentially the same in the two lipoamide dehydrogenases.

There is, however, a 1.6 Å shift in the mutual position of the two subunits, which does not affect the geometry of the catalytic center (Fig. 10). When the entire dimers of the two enzymes are superimposed, the rms difference for 482 C_α atoms is 1.25 Å, only marginally higher than the values observed in the single domain superpositions.

The results of the comparison between LipDH Val and glutathione reductase are shown in Table VI. The FAD-binding domains of subunit A were superimposed and, after that, the additional rotation and translation operations required for the optimal superpositions of every single domain as well as of the entire subunit B were calculated. The procedure is the same as used for the analysis of *A. vinelandii* LipDH and the results match quite closely those previously obtained.[5] Only a few differences need to be discussed.

1. A larger rotation in LipDH Val than in *A. vinelandii* LipDH seems to be required for the optimal superposition of the central domain (D3). However, the relatively small variation in the rms difference before and after superposition suggests that this dif-

TABLE VI. Comparison Between the Structures of Lipoamide Dehydrogenases and Glutathione Reductase*

	rms†									
	Before	After	$N_{c\alpha}$‡	K§	ϕ	ψ	Tx**	Ty	Tz	T††
D1§§										
Azo‡‡		0.87	88							
Val		1.00	89							
D2										
Azo	2.39	0.96	72	7.3	61	65	−0.5	−0.4	−1.7	1.8
Val	2.10	1.19	70	5.1	37	85	−0.3	−0.2	−1.3	1.5
D3										
Azo	0.94	0.62	25	1.9	80	70	−0.4	0.0	0.5	0.6
Val	1.09	0.62	25	6.1	35	53	−0.5	0.3	0.3	0.5
D4										
Azo	3.22	1.42	61	7.8	317	59	−2.0	0.9	−0.7	2.3
Val	3.01	1.11	60	6.4	28	42	−2.1	0.4	−0.6	2.4
sB										
Azo	3.89	1.32	246	4.4	32	45	−3.8	2.7	1.3	4.8
Val	4.00	1.38	238	8.0	53	72	−6.4	5.0	−0.9	7.6

*The coordinates set 3GRS from the protein data bank was used.[6]
†rms difference before and after optimal superposition.
‡$N_{c\alpha}$, number of atoms used in the superposition. Only C_α atoms of the secondary structure residues (Fig. 1) were employed.
§K,ϕ,ψ, polar rotation angles as defined by Rossmann and Blow.[42]
**Tx Ty Tz, translation (Å) along the three cartesian axes, when the rotation axis passes through the center of domains or subunits used in the superposition.
††T, absolute value of the translation vector.
‡‡The comparison was made by first superimposing the FAD-binding domain of the A subunit of glutathione reductase onto the same domain of LipDH Val ('VAL') and of *A. vinelandii* LipDH ('AZO'). Subsequently, the additional operations required for the best superpositions of every single domain and of the opposite chain (subunit B) were calculated. For the superpositions the method of Rao and Rossmann[41] was used.
§§D1, D2, D3, D4, sB, FAD-binding, NAD-binding, central, interface domains and subunit B, respectively.

ference is mainly due to the small number of the atoms used and not a real change in the orientation of central domain with respect to the FAD-binding domain.

2. The similarity between the interface domain (D4) of LipDH and glutathione reductase is higher in the case of LipDH Val than in *A. vinelandii* LipDH.

3. Finally, the modification observed in the dimer organization becomes even more pronounced in LipDH Val, with a shift in the mutual position of the two subunits larger than 7 Å, when comparing LipDH Val and glutathione reductase.

We can therefore conclude that the structure of LipDH Val confirms what was the most striking result of the comparison between lipoamide dehydrogenase and glutathione reductase. The changes in the tertiary and quaternary structures do not affect the catalytic center, which in glutathione reductase and both lipoamide dehydrogenases is virtually identical. Very recently, similar observations have been reported also for other members of the family of the disulfide oxidoreductases, like mercuric reductase,[43] trypanothione reductase,[44] and thioredoxin reductase.[45] What we are observing seems indeed to be a quite complicated way to preserve the geometry of the most precious part of an enzyme, its catalytic center.

ACKNOWLEDGMENTS

We thank A. Schierbeek for his initial contributions to this project. The discussions with J. Benen, W. van Berkel, and A. de Kok (University of Wageningen, the Netherlands) about the catalytic and biochemical properties of lipoamide dehydrogenase have been very stimulating. It is a pleasure to thank Dr. B. Dijkstra and the other members of the Groningen Protein Crystallography for advice and assistance regarding some computing problems. This research was supported by the Netherlands Foundation for Chemical Research (SON) with financial aid from the Netherlands Organization for Scientific Research (NWO) and USPHS Grant GM 30428.

REFERENCES

1. Williams C.H. Jr. Lipoamide dehydrogenase, glutathione reductase, thioredoxin reductase and mercuric reductase-family of flavoenzyme transhydrogenases. In: "Chemistry and Biochemistry of Flavoenzymes." Müller, F. (ed.). Boca Raton, FL: CRC Press, in press, 1992.
2. Danson, M.J. Dihydrolipoamide dehydrogenase: a 'new' function for an old enzyme? Biochem. Soc. Trans. 16:87–89, 1988.
3. Danson, M.J., Conroy, K., McQuattie, A., Stevenson, K.J.

Dihydrolipoamide dehydrogenase from *Trypanosoma brucei*. Biochem. J. 243:661–665, 1987.
4. Schierbeek, A.J., Swarte, M.B.A., Dijkstra, B.W., Vriend, G., Read, R.J., Hol, W.G.J., Drenth, J., Betzel, C. X-ray structure of lipoamide dehydrogenase from *A. vinelandii* determined by a combination of molecular and isomorphous replacement techniques. J. Mol. Biol. 206:365–379, 1989.
5. Mattevi, A., Schierbeek, A.J., Hol, W.G.J. The refined crystal structure of *Azotobacter vinelandii* lipoamide dehydrogenase at 2.2 Å resolution. A comparison with the structure of glutathione reductase. J. Mol. Biol., 220:975–994, 1991.
6. Karplus, P.A., Schulz, G.E. Refined crystal structure of glutathione reductase at 1.54 Å resolution. J. Mol. Biol. 195:701–729, 1987.
7. Benen, J.A.E., Van Berkel, W.J.H., de Kok, A. site-directed mutagenesis studies on lipoamide dehydrogenase from *Azotobacter vinelandii*. In: "Flavins and Flavoproteins." Curti, B., Zanetti, G., Ronchi, S. (eds.). Berlin: Walter de Gruyter, 557–564, 1991.
8. Sokatch, J.R., McCully, J., Roberts, C.M. Purification of a branched-chain ketoacid dehydrogenase from *P. putida*. J. Bacteriol. 148:647–652, 1981.
9. Burns, G., Brown, T., Hatter K., Sokatch J.R. Sequence analysis of the lpdV gene for lipoamide dehydrogenase of branched-chain-oxoacid dehydrogenase of *Pseudomonas putida*. Eur. J. Biochem. 179:61–69, 1989.
10. Thieme, R., Pai, E.F., Schiermer, R.H., Schulz, G.E. The three-dimensional structure of glutathione reductase at 2.0 Å resolution. J. Mol. Biol. 152:763–782, 1981.
11. Priestle, J.P. A stereocartoon drawing program for proteins. J. Appl. Crystallogr. 21:515–537, 1988.
12. Matthews, B.W. Solvent content in protein crystals. J. Mol. Biol. 33:493–497, 1968.
13. Machin, P.A., Wonacott, A.J., Moss, D. Daresbury Lab. News 10:3–9, 1983.
14. Crowther, R.A. The fast rotation function: In: "The Molecular Replacement Method." Rossmann, M.G. (ed.). Int. Sci. Rev. Ser. 13. New York: Gordon & Breach, 1972:173–178, 1972.
15. Crowther, R.A., Blow, D.M. A method of positioning a known molecule in an unknown crystal structure. Acta Crystallogr. 23:544–548, 1967.
16. Tronrud, D.E., Ten Eyck, L., Matthews, B.W. An efficient general-purpose lease squares refinement program for macromolecular structures. Acta Crystallogr. A43: 489–501, 1987.
17. Vriend, G. WHAT IF: A molecular modeling and drug design program. J. Mol. Graphics 8:52–56, 1990.
18. Fujinaga, M., Gros, P., van Gunsteren, W.F. Testing the method of crystallographic refinement using molecular dynamics. J. Appl. Crystallogr. 22:1–8, 1989.
19. Gros, P., Betzel, C., Dauter, Z., Wilson, K.S., Hol, W.G.J. Molecular dynamics refinement of a thermitase-eglin-c complex at 1.98 Å resolution and comparison of two crystal forms that differ in calcium content. J. Mol. Biol. 210:347–367, 1989.
20. Hall, S.R., Stewart, J.M. Editors of XTAL2.2 User's manual. Universities of Western Australia and Maryland, 1987.
21. Read, R.J. Improved Fourier coefficients for maps using phases from partial structures with errors. Acta Crystallogr. A42:140–149, 1986.
22. Jones, T.A. A graphics model building and refinement system for macromolecules. J. Appl. Crystallogr. 11:155–164, 1978.
23. Kabsch, W., Sander, C. Dictionary of protein secondary structure: pattern recognition of hydrogen-bonded and geometrical features. Biopolymers 22:2577–2637, 1983.
24. Ramachandran, G.N., Ramakrishnan, C., Sasisekharan, V. Stereochemistry of polypeptide chain configurations. J. Mol. Biol. 7:95–99, 1963.
25. Bystroff, C., Oatley, S.J., Kraut, J. Crystall structures of *Escherichia coli* dihydrofolate reductase: the NADP$^+$ holoenzyme and the folate-NADP$^+$ ternary complex. Substrate binding and a model for the transition state. Biochemistry 29:3263–3277, 1990.
26. Chothia, C., Lesk, A.M. The relation between the divergence of sequence and structure in proteins. EMBO J 5: 823–826, 1986.
27. Wierenga, R.K., Drenth, J., Schulz, G.E. Comparison of the three-dimensional structure of the FAD-binding domain of p-hydroxybenzoate hydroxylase with the FAD- as well NADPH-binding domains of glutathione reductase. J. Mol. Biol. 167:725–739, 1983.
28. Carothers D.J., Pons G., Patel M.Dihydrolipoamide dehydrogenase: functional similarities and divergent evolution of the pyridine nucleotide-disulphide oxidoreductases. Arch. Biochem. Biophys. 2:409–425, 1989.
29. Rice, D.W., Schulz, G.E., Guest, J.R. Structural relationship between glutathione reductase and lipoamide dehydrogenase. J. Mol. Biol. 174:483–496, 1984.
30. Pai, E.F., Schulz G.E. The catalytic mechanism of glutathione reductase as derived from X-ray diffraction analyses of reaction intermediates. J. Biol. Chem. 25:1753–1757, 1982.
31. Pai, E.F., Karplus, P.A., Schulz G.E. Crystallographic analysis of the binding of NADPH, NADPH fragments, and NADPH analogues to glutathione reductase. Biochemistry 27:4465–4474, 1988.
32. Arnott, S., Hukins, D.W. Conservation of conformation in mono and poly-nucleotides. Nature (London) 224:886–888, 1969.
33. Rossmann, M.G., Moras, D., Olsen K.W. Chemical and biological evolution of a nucleotide-binding protein. Nature (London) 250:194–199, 1974.
34. Lindqvist, Y., Branden, C., Mathews, F.S., Lederer, F. Spinach glycolate oxidase and yeast flavocytochrome b_2 are structurally homologous and evolutionarily related enzymes with distinctly different function and flavin mononucleotide binding. J. Biol. Chem. 266:3198–3207, 1991.
35. Scrutton, N.G., Berry, A., Perham R.N. Redesign of the coenzyme specificity of a dehydrogenase by protein engineering. Nature (London) 343:38–43, 1990.
36. Wierenga, R.K., Terpstra, P., Hol, W.G.J. Prediction of occurence of the ADP-binding βαβ-fold in proteins, using an amino acid sequence fingerprint. J. Mol. Biol. 187:101–107, 1986.
37. Karplus, P.A., Schulz, G.E. Substrate binding and catalysis by glutathione reductase as derived from refined enzyme:substrate crystal structures at 2 Å resolution. J. Mol. Biol. 210:163–180, 1989.
38. Karplus, P.A., Daniels, M., Herriott, J.R. Atomic structure of ferredoxin-NADP$^+$ reductase: Prototype for a structurally novel flavoenzyme family. Science 251:60–66, 1991.
39. Berry, A., Scutton, N.S., Perham R.N. Switching kinetic mechanism and putative proton donor by directed mutagenesis in glutathione reductase. Biochemistry 28: 1264–1269, 1989.
40. Yorita, K.M., Massey, V., Williams, C.H. Properties of lipoamide dehydrogenase from *E. coli* modified by site-directed mutagenesis: K53R and I184Y. In: "Flavins and Flavoproteins." Curti, B., Zanetti, G., Ronchi, S. (eds). Berlin: Walter de Gruyter, 303–309, 1991.
41. Rao, S.T., Rossmann, M.G. Comparison of super-secondary structures in proteins. J. Mol. Biol. 76:241–256, 1973.
42. Rossmann, M.G., Blow, D.M. The detection of sub-units within the crystallographic asymmetric unit. Acta Crystallogr. 15:23–31, 1962.
43. Schiering, N., Kabsch, W., Moore, M.J., Distefano, M.D., Walsh, C.T., Pai, E.F. Structure of the detoxification catalyst mercuric ion reductase from *Bacillus* sp. strain RC607. Nature (London) 352:168–172, 1991.
44. Kuriyan, J., Kong, X.P., Krishna, T.S.R., Sweet, R.M., Murgolo, N.H., Field, H., Cerami, A., Henderson, G.B. X-ray structure of trypanothione reductase from *Crithidia fasciculata* at 2.4 Å resolution. Proc. Natl. Acad. Sci. U.S.A. 88:8764–8768, 1991.
45. Kuriyan, J., Krishna, T.S.R., Wong, L., Guenther, B., Pahler, A., Williams, C.H., Model, P. Convergent evolution of similar function in two structurally divergent enzymes. Nature (London) 352:172–174, 1991.